DIRECT SIMULATION OF THE KINEMATIC EVOLUTION OF A POPULATION OF RIGID FIBERS

R. Mezher*[1], E. Abisset-Chavanne[1], J. Férec[2], G. Ausias[2], F. Chinesta[1]

[1]*Institut de Recherche GeM, Ecole Centrale de Nantes, 1 rue de la Noe, BP 92101, 44321 Nantes Cedex 3, France*
[2]*Université de Bretagne-Sud, EA 4250, LIMATB, 56100 Lorient, France*
* *Corresponding Author: rabih.mezher@ec-nantes.fr*

Keywords: fiber suspensions, direct simulations, microscopic description, concentrated regime.

Abstract
In this work a numerical simulation of fiber suspensions in transient and steady shear flow is presented. Concentrated suspensions are considered along with interactions between fibers: short-range hydrodynamic interaction via lubrification forces, contact forces and hydrodynamic forces. The kinematic of a population of fibers is then calculated using a derived equation of the second order orientation tensor. This simulation is necessary for rigid fiber filled composites, since the final orientation of the fibers is induced by the flow during the processing of the composites and is hard to control.

1. Introduction

Fiber suspensions have become an important part of the composite industry. In fact, most of thermoplastic and polymeric materials have poor mechanical properties and they are often reinforced with fibers. To be efficient, fibers must be oriented in the correct direction. Moreover, the content of fibers in fiber reinforced composites is generally large, and concentrated suspensions are usually considered.

Models for describing the behaviour of dilute or semi-dilute solutions of rigid short fibers exist in the litterature [1, 2]. However the behaviour of concentrated suspensions is diffcult to describe. One way of studying the behaviour of concentrated suspensions, is to perform direct numerical simulations (DNS). DNS is based on the computation, in a representative volume, of the motion of a hundred of fibers and their interactions. It is a step by step process which derives kinematics as well as macroscopic properties (i.e stresses), while taking into account the forces applied on each fiber at the the microsopic scale [3]. This method has been used for non spherical particles and for non-rigid particles under simple shear flow [4, 5]. However in these publications, all particles had the same aspect ratio, and they all flipped at the same time in the flow, thus producing large periodic fluctuations [6, 7], and making it impossible to get a reasonable steady state.

In this work the objective is to describe the kinematic of a population of rigid fibers, having a distribution of lengths. In fact, the assumption of fibers with a distribution of lengths is close to real industrial composites [8, 9].

2. Approach

In order to study the behaviour of a population of fibers in a given volume, a reference cell is considered containing a certain number of fibers (Figure 1). Periodic boundary conditions are applied to simulate fiber motion [10]. For a population of fibers, the orientation tensor $\mathbf{a_2}$ desribes the state of orientation for a population of fibers whose components are given, for a quantity of n fibers by [11]:

$$\mathrm{a}_{ik} = \frac{1}{n}\sum_{\alpha=1}^{n} p_i^{\alpha} p_k^{\alpha} \tag{1}$$

where p_i and p_k are the components of $\mathbf{p}$: the orientation of each fiber which is a unit vector. Index α indicates the number of the fiber.

The interaction tensor $\mathbf{b_2}$ is related to the probability of contact for two fibers α and β. This tensor is given by [12]:

$$\mathrm{b}_{ik} = \frac{1}{n^2}\sum_{\alpha=1}^{n}\sum_{\beta=1}^{n} |\mathbf{p}^{\alpha} \times \mathbf{p}^{\beta}| p_i^{\alpha} p_k^{\alpha} \tag{2}$$

2.1. Hypotheses

The main hypotheses made are:
(a) The matrix is Newtonian and the inertia of fibers is neglected.
(b) The fiber suspension is concentrated.
(c) Initially, the fibers are uniformly distributed in the volume, their orientation state defined by equation (1) is isotropic, and they are not in any state of contact.
(d) Fibers are assumed to be rigid prolate spheroids with lengths $l^{(i)}$, diameter d and aspect ratio $r^{(i)} = \dfrac{l^{(i)}}{d}$, with negligible mass.
(e) For the interactions between fibers, two main forces are considered: a lubrification force occurs when two fibers move close to each other and a contact force takes place when two fibers are touching one another. The shearing lubrification force is supposed to be much smaller than the squeezing one, the surface of the fibers is smooth and the friction force is small when fibers get into contact. This is why, only normal components of forces to the fiber's axis are taken into account here.

2.2. Distance between two fibers

The normal to the plane of two fibers i and k with orientations $\mathbf{p}^{(i)}$ and $\mathbf{p}^{(k)}$ is defined as:

$$\mathbf{n}^{(i,k)} = \pm\frac{\mathbf{p}^{(i)} \times \mathbf{p}^{(k)}}{\| \mathbf{p}^{(i)} \times \mathbf{p}^{(k)} \|} \tag{3}$$

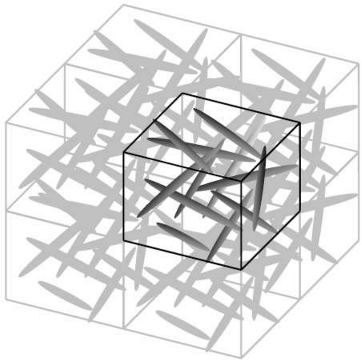

Figure 1. Reference cell surrounded by neighoring cells

The distance from the mass center of fiber i to the contact point of fiber k is $l^{(i,k)}$ and the distance from the mass center of fiber k to the contact point of fiber i is $l^{(k,i)}$ (figure 2) [13]:

$$l^{(i,k)} = \frac{-(\mathbf{r}^{(i)} - \mathbf{r}^{(k)}).\mathbf{p}^{(i)} + \left[(\mathbf{r}^{(i)} - \mathbf{r}^{(k)}).\mathbf{p}^{(k)}\right].\left(\mathbf{p}^{(i)}.\mathbf{p}^{(k)}\right)}{1 - (\mathbf{p}^{(i)}.\mathbf{p}^{(k)})^2} \tag{4}$$

$$l^{(k,i)} = \frac{-(\mathbf{r}^{(k)} - \mathbf{r}^{(i)}).\mathbf{p}^{(k)} + \left[(\mathbf{r}^{(k} - \mathbf{r}^{(i)}).\mathbf{p}^{(i)}\right].\left(\mathbf{p}^{(k)}.\mathbf{p}^{(i)}\right)}{1 - (\mathbf{p}^{(i)}.\mathbf{p}^{(k)})^2} \tag{5}$$

$\mathbf{r}^{(i)}$ being the position of the center of gravity of fiber i. Using equations (4) and (5) the gap $\chi^{(i,k)}$

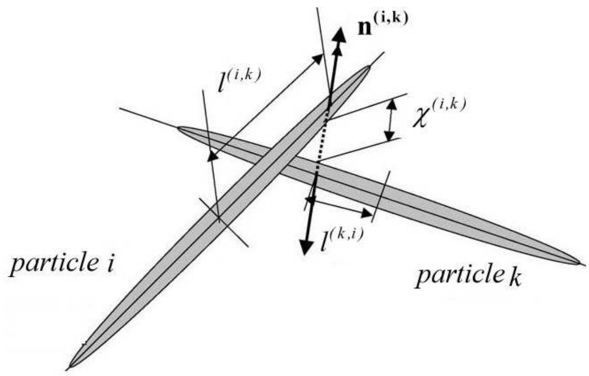

Figure 2. Contact or lubrification between two fibers

between two fibers is obtained according to [13]:

$$\chi^{(i,k)} = (\mathbf{r}^{(i)} - \mathbf{r}^{(k)}).\mathbf{n}^{(i,k)} - \frac{d}{2}\sqrt{1 - 4\frac{l^{(i,k)^2}}{l^{(i)^2}}} - \frac{d}{2}\sqrt{1 - 4\frac{l^{(k,i)^2}}{l^{(k)^2}}} \tag{6}$$

When the gap between fibers i and k is positive but smaller than a fraction of the fiber diameter d, the lubrification force is assumed to occur. On the other hand if $\chi^{(i,k)}$ is smaller than or equal to zero, the contact force occurs.

2.3. Equations of motion

A simple shear flow, having a shear rate of $\dot{\gamma}$ (unit s^{-1}) is supposed to be applied to the suspending fluid, being the velocity field given by:

$$\mathbf{u}^T(\mathbf{x}) = (\dot{\gamma}.y, 0, 0) \tag{7}$$

The flow is imposed in the first direction $x.\boldsymbol{\delta}_x$ (where $\boldsymbol{\delta}_x$ is a unit vector), of the three dimensional space $[x, y, z]$, and $\dot{\gamma}$ is supposed to be uniform in the cell. The rate of strain tensor and vorticity tensor are:

$$\mathbf{D} = \frac{1}{2}\left(\nabla\mathbf{u} + (\nabla\mathbf{u})^T\right) = \begin{bmatrix} 0 & \frac{\dot{\gamma}}{2} & 0 \\ \frac{\dot{\gamma}}{2} & 0 & 0 \\ 0 & 0 & 0 \end{bmatrix} \tag{8}$$

$$\mathbf{W} = \frac{1}{2}\left(\nabla\mathbf{u} - (\nabla\mathbf{u})^T\right) = \begin{bmatrix} 0 & \frac{\dot{\gamma}}{2} & 0 \\ -\frac{\dot{\gamma}}{2} & 0 & 0 \\ 0 & 0 & 0 \end{bmatrix} \tag{9}$$

with the velocity gradient defined as :

$$\nabla\mathbf{u} = \frac{\partial u_m}{\partial x_n} = \begin{bmatrix} 0 & \dot{\gamma} & 0 \\ 0 & 0 & 0 \\ 0 & 0 & 0 \end{bmatrix} \tag{10}$$

m=1, 2 and 3 defines the index for the three components of $\mathbf{u}(\mathbf{x})$, and n=1,2 and 3 defines the index for the three dimensions x, y, and z.

To describe the fibers motion, $\mathbf{r}^{(i)}$ is related to the fiber's perturbed velocity $\dot{\mathbf{q}}^{(i)}$ by:

$$\dot{\mathbf{r}}^{(i)} = \dot{\mathbf{q}}^{(i)} + \dot{\gamma} y^{(i)} \boldsymbol{\delta}_x \tag{11}$$

The fiber's motion is then represented by the following equation:

$$\mathbf{F}^{(i)} + \boldsymbol{\zeta}^{(i)}.\dot{\mathbf{q}}^{(i)} = 0 \tag{12}$$

where $\mathbf{F}^{(i)}$ represents the resultant force acting on fiber i and $\boldsymbol{\zeta}^{(i)}$ is the resistance tensor of the fiber in the shear flow [14]. $\mathbf{F}^{(i)}$ is the sum of the lubrification and contact forces acting on the fiber. The evolution of the fiber's orientation is:

$$\dot{\mathbf{p}} = -\mathbf{p}^{(i)} \times \left(\omega^{(i)} - \boldsymbol{\Omega}\right) \tag{13}$$

where $\boldsymbol{\Omega}$ is the fluid's angular velocity. Equation (13) contains a new vector $\omega^{(i)}$, which is the relative rotating velocity of the fiber with respect to the fluid. Since the inertia of fibers is neglected, the balance of momentum writes:

$$\mathbf{T}^{(i)} + \boldsymbol{\xi}.\omega^{(i)} + \boldsymbol{\varsigma} : \mathbf{D} = 0 \tag{14}$$

where $\mathbf{T}^{(i)}$ is the resultant momentum of the forces, $\boldsymbol{\xi}$ and $\boldsymbol{\varsigma}$ are the rotating resistance tensors [14]. The last term in equation (14) is the torque caused by the fluid's deformation. For a couple of fibers in interaction $\mathbf{T}^{(i)}$ is given by:

$$\mathbf{T}^{(i)} = \mathbf{p}^{(i)} \times \left(\sum_{k \neq i} l^{(i,k)}.F_c^{(i,k)} \mathbf{n}^{(i,k)} + \sum_{l \neq i} l^{(i,l)}.F_{lb}^{(i,l)} \mathbf{n}^{(i,l)} \right) \tag{15}$$

Index k represents each fiber in contact with fiber i and index l represents each fiber in lubrification with fiber i. $F_c^{(i,k)}$ and $F_{lb}^{(i,l)}$ are the contact and lubrification forces respectively. Finally from equations (14) and (15) equation (13) can be rewritten as:

$$\dot{\mathbf{p}}^{(i)} = \beta\left(\sum_{k\neq i} l^{(i,k)}.F_c^{(i,k)}\mathbf{n}^{(i,k)} + \sum_{l\neq i} l^{(i,l)}.F_{lb}^{(i,l)}\mathbf{n}^{(i,l)}\right) + \dot{\mathbf{p}}_{jef}^{(i)} \tag{16}$$

where β is a constant and the Jeffery orientation evolution for a fiber with no interactions is given by:

$$\dot{\mathbf{p}}_{jef}^{(i)} = \mathbf{\Omega}.\mathbf{p}^{(i)} + \lambda^{(i)}\left[\mathbf{D}.\mathbf{p}^{(i)} - \left(\mathbf{D} : \mathbf{p}^{(i)} \otimes \mathbf{p}^{(i)}\right).\mathbf{p}^{(i)}\right] \tag{17}$$

where $\lambda^{(i)}$ is a parameter that depends on the aspect ratio of the fiber i.

3. Results and Discussion

3.1. Initial state

A volume fraction of fibers of 11.5% was used to create the initial state. A total number of $n = 343$ fibers were placed into a cubic volume (figure 3) according to hypothesis (c). Their isotropic state was verified by applying equation (1), thus initially one gets: $\mathbf{a_2} \simeq \frac{1}{3}\mathbf{I}$ and $\mathbf{b_2} \simeq \frac{\pi}{12}\mathbf{I}$. $\mathbf{I}$ being the unit tensor. A normal distribution function was used to create fibers with varying lengths. This distribution was associated with a mean aspect ratio of 20 and a standard deviation of 3.

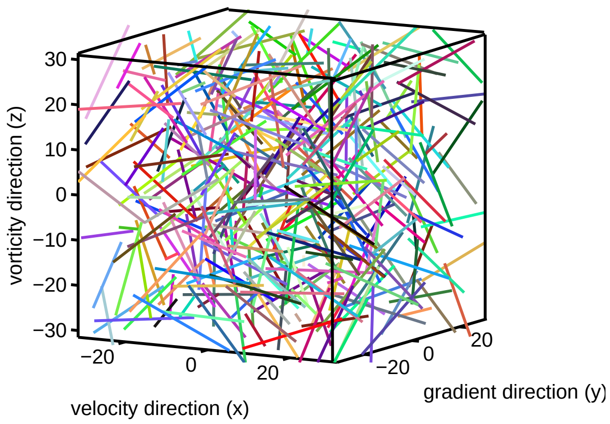

Figure 3. Initial state of the fibers

3.2. Kinematic evolution with interactions

A simple shear flow, with a shear rate $\dot{\gamma} = 1\,s^{-1}$ was applied in the suspensions depicted in figure 3. Figure 4 shows the evolution of the $a_{11} = a_{xx}$ component. The dotted curve shows this evolution for a polydisperse concentrated suspension. From figure 4 it is possible to determine the transient phase and an almost steady phase in the region between 100 and 200 seconds where the a_{11} component no longer changes. The width of the first peak and the fluctuations that occur

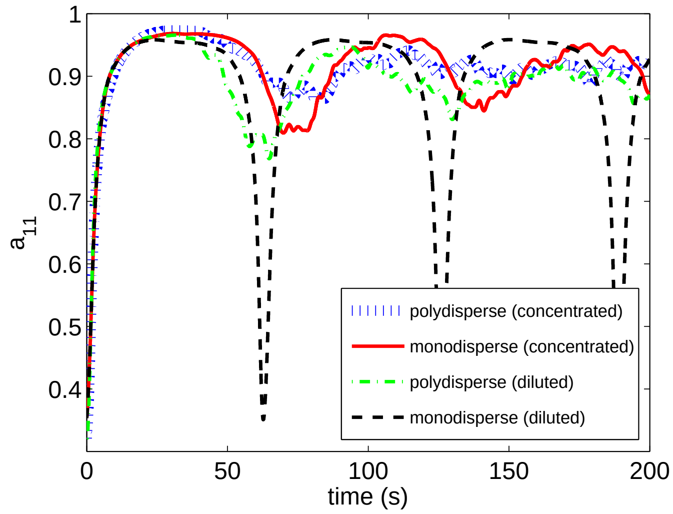

Figure 4. Time evolution of the a_{11} component

in the steady state, are due to the amount of interactions happening between fibers (contact and lubrification forces).

Unlike the case of diluted suspensions (in absence of interactions) where fibers having the same lengths rotated periodically with the flow [15, 16] (dashed curve in figure 4), these interactions tend to slow down the rotation of the fibers and alter the periodic Jeffery's orbit. Finally the fibers reach an orientation close to the direction of the applied shear flow (figure 5). Also for polydisperse diluted suspensions (dotted dashed curve), the Jeffery's orbit is again changed because fibers don't have the same aspect ratio (parameter $\lambda^{(i)}$ in equation (17)). Thus each fibers will have a different speed of rotation and no periodic behaviour is observed.

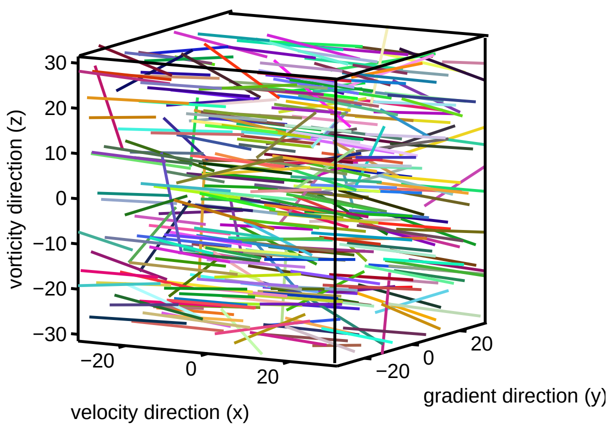

Figure 5. Final state of the fibers

Equation (2) from which the b_{11} component is calculated, describes the interactions occuring. From figure 6, a transient and an almost steady state are also noticed in the polydisperse concentrated case (dotted curve) for approximately the same time zone: the steady phase is in the same region as the one in figure 4, confirming the fact that the interactions become stable with the fibers aligning in a direction very close to that of the applied shear flow. For the monodisperse concentrated case (solid curve), an almost periodic behaviour is observed along with a decreasing amplitude. This is due to the fact that in the polydisperse case longer fibers exist which lead to an increase in the number of contacts. Thus the interactions in the polydisperse case become stable in a shorter time than those in the monodisperse case where fibers are more likely to rotate. In fact figure 4 (solid curve), shows that in the region between 100 and 200 seconds, the fibers tend to rotate rather than being in a steady state. For the monodisperse diluted case there are no interactions, hence the b_{11} component is equal to zero. This is why the monodisperse diluted case isn't represented here.

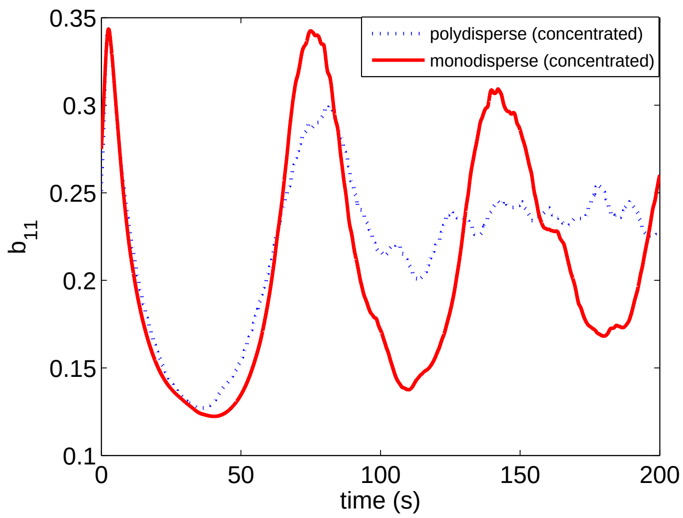

Figure 6. Evolution of the b_{11} component with time

4. Conclusion

In this work a DNS of a population of fibers was conducted in order to study the interactions involved. Unlike diluted suspensions with fibers having the same length, it was shown from the evolution of the a_{11} component that polydisperse concentrated suspensions of fibers exhibit two phases: a transient phase where the fibers tend to rotate but are slowed down by the interactions involved and an almost steady state represented by the majority of the fibers aligned in the flow shear direction. In this direction interactions are stable and that was shown by the evolution of the b_{11} component. For the monodisperse concentrated case, the interactions take a longer time to become stable and are fluctuating with a decreasing amplitude, along with fibers that tend to rotate. The difference between the two cases, was due to the existence of longer fibers in the polydisperse case, that increased contacts between fibers. Finally for the polydisperse diluted suspensions, the periodic Jeffery's orbit was altered because fibers had different aspect ratios.

The next step of this work is to compare these results with the prediction of the kinetic theory and to derive rheological properties.

References

[1] F. P. Folgar and C. L. Tucker. Orientation behavior of fibers in concentrated suspensions.

Journal of Reinforced Plastic Composites, volume 3:99, 1984.

[2] G. B. Jeffery. The motion of ellipsoidal particles immersed in a viscous fluid. *Proceedings Royal Society*, volume A102(161), 1922.

[3] G. Ausias, X. J. Fan, and R. I. Tanner. Direct simulations for concentrated fiber suspensions in transient and steady state shear flows. *Journal of Non-Newtonian Fluid Mechanics*, volume 135:46–57, 2006.

[4] X. J. Fan, N. Phan-Thien, and R. Zheng. A direct simulation of fiber suspensions. *Journal of Non-Newtonian Fluid Mechanics*, volume 74:113–135, 1998.

[5] C. F. Schmid, L. H. Switzer, and D. J. Klingenberg. Simulations of fiber flocculation: effects of fiber properties and interfiber friction. *Journal of Rheology*, volume 44(4):781–809, 2000.

[6] S. Yamamoto and T. Matsuoka. Dynamic simulation of a platelike particle dispersed system. *Journal of Chemical Physics*, volume 107(8):3300–3308, 1997.

[7] C. Pozrikidis. Orientation statistics and effective viscosity of suspensions of elongated particles in simple shear flow. *European Journal of Mechanics B/Fluids*, volume 24:125–136, 2005.

[8] C. Mobuchon. Propriétés rhéologiques en cisaillement et en élongation d'un polypropylène chargé de fibres de verre courtes. Master's thesis, Ecole Polytechnique de Montréal, 2002.

[9] C. Mobuchon, P. J. Carreau, M. C. Heuzey, M. Sepehr, and G. Ausias. Shear and extensional properties of short glass fiber reinforced polypropylene. *Polymer Composites*, volume 26(3):247–263, 2005.

[10] G. Bossis, A. Meunier, and J. D. Sherwood. Stokesian dynamics simulations of particle trajectories near a plane. *Physics of Fluids a-Fluid Dynamics*, volume 3(8):1853–1858, 1991.

[11] S. G. Advani and C. L. Tucker. The use of tensors to describe and predict fiber orientation in short fiber composites. *Journal of Rheology*, volume 31(8):751–784, 1987.

[12] J. Férec, G. Ausias, M. C. Heuzey, and P. J. Carreau. Modeling fiber interactions in semiconcentrated fiber suspensions. *Journal of Rheology*, volume 53(1):49–72, 2009.

[13] Y. Yamane, Y. Kaneda, and M. Doi. Numerical-simulation of semidilute suspensions of rodlike particles in shear-flow. *Journal of Non Newtonian Fluid Mechanics*, volume 54:405–421, 1994.

[14] S. Kim and S. J. Karrila. *Microdynamics: Principles and Selected Applications*. ButterworthHeinemann, Boston, 1991.

[15] S. Yamamoto and T. Matsuoka. A method for dynamic simulation of rigid and flexible fibers in a flow field. *Journal of Chemical Physics*, volume 98(1):644–650, 1993.

[16] S. Yamamoto and T. Matsuoka. Dynamic simulation of microstructure and rheology of fiber suspensions. *Polymer Engineering and Science*, volume 36(19):2396–2403, 1996.